Sensors and Actuators B 224 (2016) 833–840

Contents lists available at ScienceDirect

Sensors and Actuators B: Chemical

journal homepage: www.elsevier.com/locate/snb

Flexibility and electrical and humidity-sensing properties of *N*-substituted pyrrole derivatives and composite films of Au nanoparticles/*N*-substituted pyrrole derivatives

Pi-Guey Su*, Sih-Ru Chiu, Yu-Te Lin

Department of Chemistry, Chinese Culture University, Taipei 111, Taiwan

ARTICLE INFO

Article history:
Received 8 August 2015
Received in revised form 21 October 2015
Accepted 22 October 2015
Available online 27 October 2015

Keywords:
Humidity sensor
N-substituted pyrrole derivatives
Gold nanoparticles
Composite

ABSTRACT

Novel impedance-type humidity sensors were fabricated by coating 2,5-dimethyl-1-phenyl-1*H*-pyrrole (**1**), 1-(4-aminophenyl)-2,5-dimethyl-1*H*-pyrrole (**2**), 1-(4-nitrophenyl)-2,5-dimethyl-1*H*-pyrrole (**3**) and gold nanoparticles/compound **3** (AuNPs/compound **3**) composite films on alumina and plastic substrates. Compound **1**, compound **2**, compound **3** and AuNPs/compound **3** composite films were analyzed using atomic force microscopy (AFM) and UV–vis spectroscopy. The effects of the substituents on the benzene ring of compound **1** on the electrical and humidity-sensing properties of the compound **1** film were studied. The humidity sensor that was fabricated with the compound **3** exhibited high sensitivity but a higher resistance at low humidity than that which was made of the compound **1**. The effects of the AuNPs on the electrical and humidity sensing properties of the AuNPs/compound **3** composite film on a PET substrate were investigated. The sensor that was made of the AuNPs/compound **3** composite film exhibited high sensitivity, good linearity, small hysteresis, high flexibility, a short response/recovery time, a weak dependence on temperature and high long-term stability. The linearity of the humidity sensor depended on the applied frequency. The sensing mechanism of the AuNPs/compound **3** composite film was elucidated with reference to impedance plots.

© 2015 Elsevier B.V. All rights reserved.

1. Introduction

Humidity sensors are extensively utilized in the measurement and control of humidity for the purposes of human comfort and for many industrial processes. Therefore, a high-performance humidity sensor must have many characteristics, including a linear response, small hysteresis, high sensitivity, short response time, low power consumption, chemical and physical stability, a wide operating range of humidity and low cost. Materials that have been examined for this purpose include polymers and ceramics, which have their own advantages and conditions of application [1–4]. Polymeric sensors have attracted great interest for measuring humidity because they are light-weight, flexible, and low-cost and they have a large surface area. Humidity sensors that are fabricated from polymeric materials are divided into two classes, which are impedance-type and capacitive-type [5]. Polyimides are the most studied polymeric capacitive-type sensing materials, whereas the most important impedance-type sensing materials are polymer electrolytes or conducting polymers. Of conducting polymers, polypyrrole (PPy) and its composites are the most attractive for use in humidity sensors owing to their remarkable mechanical and electrical properties, ease of synthesis and favorable environmental stability [6–14].

Recently, *N*-substituted pyrrole derivatives have become increasingly important because they have become associated with a wide range of pharmacological and biological activities [15,16]. The most common methods for synthesizing *N*-substituted pyrrole derivatives involve the Paal–Knorr condensation reaction of 1,4-diketones with amines using various catalysts such as *p*-toluenesulfonic acid [17], silica-supported antimony(III) chloride [18] and polystyrene-supported $GaCl_3$ [19]. Recently, Wu et al. [20] synthesized *N*-substituted pyrrole derivatives by the Paal–Knorr reaction in an aqueous medium with β-cyclodextrin as a catalyst. Au nanoparticles (AuNPs) have attracted considerable interest for use in chemical sensors and biosensing applications because of their attractive electronic and unique optical, thermal and physical properties, their large surface area and their catalytic activity [21]. According to our knowledge, no work has been reported to fabricate humidity sensors that are based on *N*-substituted pyrrole derivatives and AuNPs/*N*-substituted pyrrole derivative composite

* Corresponding author. Tel.: +886 2 28610511x25332; fax: +886 2 28614212.
E-mail address: spg@faculty.pccu.edu.tw (P.-G. Su).

http://dx.doi.org/10.1016/j.snb.2015.10.077
0925-4005/© 2015 Elsevier B.V. All rights reserved.

www.sp...com.cn

materials. This work elucidates the electrical and humidity-sensing characteristics, as functions of relative humidity (RH), of 2,5-dimethyl-1-phenyl-1*H*-pyrrole (**1**), 1-(4-aminophenyl)-2,5-dimethyl-1*H*-pyrrole (**2**), and 1-(4-nitrophenyl)-2,5-dimethyl-1*H*-pyrrole (**3**) films that were fabricated by a well-known Paal–Knorr reaction in aqueous media using β-cyclodextrin as a catalyst. The effect of the substituent on the benzene ring of the *N*-substituted pyrrole derivative film on its electrical and humidity-sensing properties was studied. To reduce the high resistance of the *N*-substituted pyrrole derivatives films at low humidity for practical use, composite material of AuNPs and 1-(4-nitrophenyl)-2,5-dimethyl-1*H*-pyrrole (**3**) (AuNPS/compound **3**) were prepared in this study, and the electrical and humidity sensing properties of the composite film were studied. The films were characterized by atomic force microscopy (AFM) and UV–vis spectrophotometer. The complex impedance spectra were used to elucidate the role of ions in the conductance of the composite film of AuNPS/compound **3**. The flexibility and humidity-sensing characteristics of the film, including the sensitivity, hysteresis, response time, recovery time and long-term stability, were also investigated, and the effects of the applied frequency and ambient temperature were elucidated.

2. Experimental

2.1. Materials

2–5-Hexanedione (Sigma-Aldich), aniline (Shimakyu's Pure Chemicals), *p*-nitroaniline (Alfa Aesar), *p*-phenylene diamine (Sigma-Aldrich), β-cyclodextrin (TCI), hydrogen tetrachloroaurate(III) hydrate (UniRegion Bio-Tec), sodium citrate (Shimakyu's Pure Chemicals) and polyvinylpyrrolidone (PVP, average mol wt. 40,000, Sigma-Aldich) were used without further purification. All used deionized water (DIW) was prepared using a Milli-Q Millipore (Bedford, MA, USA) purification system, and the resistivity of water was above 18.0 MΩ/cm.

2.2. Preparation of N-substituted pyrrole derivatives using Paal–Knorr reaction

The preparation of *N*-substituted pyrrole derivatives was prepared using the method in the literature [20]. 2,5-Dimethyl-1-phenyl-1*H*-pyrrole (**1**) was synthesized by mixing 2–5-hexanedione (0.6 mmol), aniline (0.5 mmol) and β-cyclodextrin (10 mol%) in H_2O (3 mL), and then stirring the mixture for 24 h at 60 °C. After the reaction had run to completion, the aqueous phase was extracted using ethyl acetate. Similar steps were followed to prepare 1-(4-aminophenyl)-2,5-dimethyl-1*H*-pyrrole (**2**), and 1-(4-nitrophenyl)-2,5-dimethyl-1*H*-pyrrole (**3**). Fig. 1 plots the chemical structure of the *N*-substituted pyrrole derivatives.

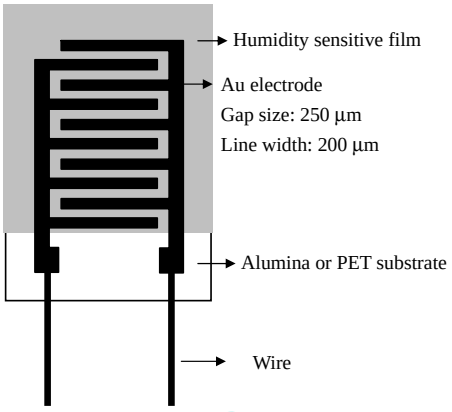

Fig. 2. Structure of humidity sensor.

2.3. Preparation of AuNPs

AuNPs was prepared using the method in the literature [22]. The AuNPs colloidal particles were prepared by adding 38.8 mM sodium citrate to boiling aqueous 1 mM $HAuCl_4$. The solution was boiled for 15 min with vigorous stirring, and then allowed to cool to room temperature, before being stored at 4 °C.

2.4. Fabrication of humidity sensors

Fig. 2 schematically depicts the structure of the humidity sensor. The interdigited gold electrodes were made on an alumina substrate by screen-printing method. The interdigited gold electrodes were made on a flexible substrate (polyethylene terephthalate; PET) by sputtering initially Cr (thickness 50 nm) and then Au (thickness 250 nm) in a temperature range of 120 to 160 °C. The electrode gap was 0.25 mm. The substrates were firstly treated with an H_2O_2/H_2SO_4 mixture (1:2, 15 mL), washed in de-ionized water (DIW) and then cleaned in acetone solution for 3 min. The precursor solution of *N*-substituted pyrrole derivatives was prepared by adding 1 mL of the as-prepared *N*-substituted pyrrole derivatives to 10 mL of DIW, and then ultrasonically vibrating the solution thus formed for approximately 0.5 h to yield a well-mixed suspension. The precursor solution of the AuNPs/compound

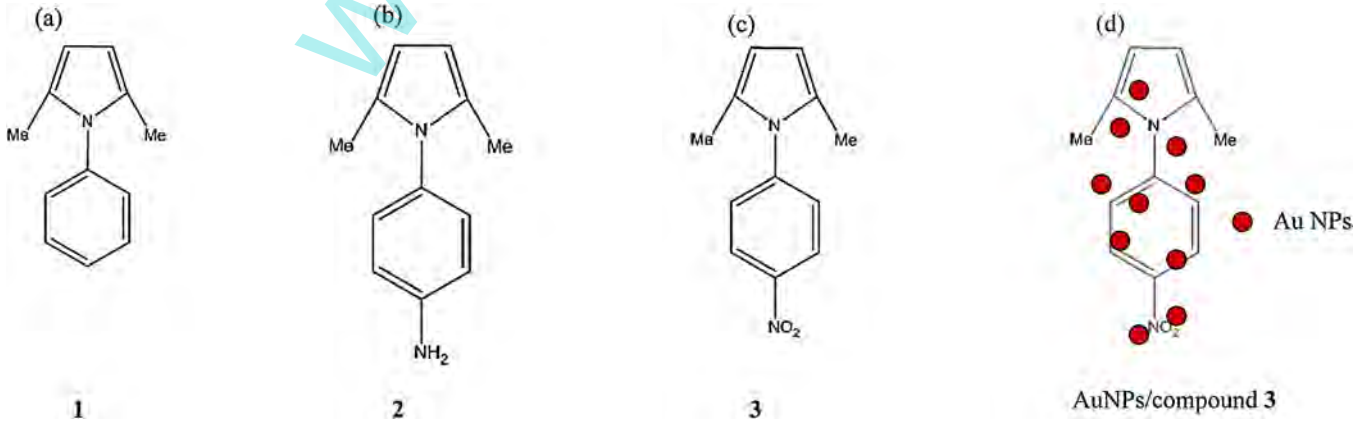

Fig. 1. Chemical structures of (a) 2,5-dimethyl-1-phenyl-1*H*-pyrrole **1**; (b) 1-(4-aminophenyl)-2,5-dimethyl-1*H*-pyrrole **2**; (c) 1-(4-nitrophenyl)-2,5-dimethyl-1*H*-pyrrole **3** and (d) AuNPs/compound **3**.

www.spm.com.cn

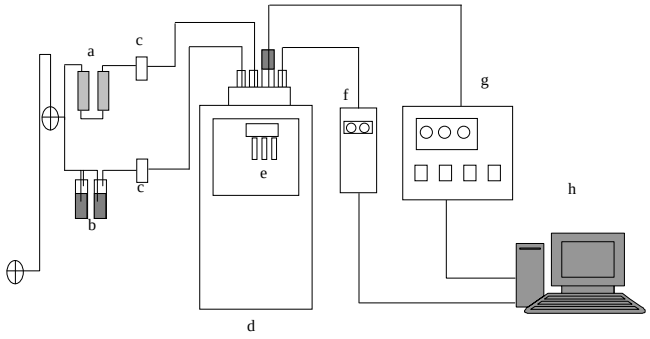

Fig. 3. Schematically plots the impedance measurement of sensors and the humidity atmosphere controller. (a) Molecular sieve and desiccating agent; (b) water; (c) mass flow controller; (d) controlled temperature detection chamber; (e) humidity sensor; (f) hygrometer; (g) LCZ meter; (h) PC.

3 nanocomposite was prepared by adding 1 mL of the as-prepared 1-(4-nitrophenyl)-2,5-dimethyl-1*H*-pyrrole **3** in aqueous media, 500 μL of the PVP (20 mg/mL) and 1 mL of the as-prepared AuNPs to 10 mL of DIW, and then ultrasonically vibrating the resulting mixture for about 0.5 h to obtain a well-mixed suspension. Then, 20 μL of the precursor solutions of *N*-substituted pyrrole derivatives and the AuNPs/compound **3** composite were drop-coated onto alumina or flexible substrates, which were then thermally treated at 60 °C for 0.5 h in air.

2.5. Instruments and analysis

The formation of AuNPs and AuNPs/compound **3** were characterized by UV–vis spectroscopy (Agilent 8453). The surface microstructure of the thin film that was coated on an alumina substrate was investigated using an atomic force microscope (AFM, Ben-Yuan, CSPM 4000) in tapping mode which the horizontal and vertical resolution are 0.26 and 0.10 nm, respectively. An infrared spectrometer (Nicolet 380) was used to obtain the IR spectra of the *N*-substituted pyrrole derivatives. The impedance of the sensor was measured as a function of RH using an LCR meter (Philips PM6306) in a test chamber under the conditions of a measurement frequency of 1 kHz, an applied voltage of 1 V, an ambient temperature of 25 °C. As shown in Fig. 3, a divided humidity generator was used as the principal facility for producing the testing gases. The required humidity was produced by adjusting the proportion of dry and humid air generated by the divided flow humidity generator under a total flow rate is 10 L/min. The model of two mass flow controller's (Hastings) and flow display power-supply used is the Protec PC-540 manufactured by Sierra Instruments Inc, as described elsewhere [23]. The RH values were measured using a calibrated hygrometer (Rotronic) with an accuracy of ±0.1% RH. Flexibility experiments were performed in which the sensor was bent to various degrees as their responses were monitored as a function of the period of exposure to humidity. The bending angle was measured using a goniometer.

3. Results and discussion

3.1. Characterization of N-substituted pyrrole derivatives and AuNPs/N-substituted pyrrole derivative composite films

3.1.1. Microstructure of surface

The surface morphologies of the compound **1**, compound **2**, compound **3** and AuNPs/compound **3** films were studied by AFM. Fig. 4 presents the AFM images of the compound **1**, compound **2**, compound **3** and AuNPs/compound **3** films on an alumina substrate. The root mean square (RMS) roughness values of the compound **1**, compound **2**, compound **3** and AuNPs/compound **3** films were 18.4, 18.7, 19.8 and 19.4 nm, respectively. The compound **1**, compound **2**, compound **3** and AuNPs/compound **3** films all had smooth surfaces with similar values of roughness. Numerous bright particles were clearly dispersed on the outer surfaces of the AuNPs/compound **3** composite film (Fig. 4(d)).

3.1.2. UV–vis spectra

Fig. 5 presents the UV–vis absorption spectra of as-prepared AuNPs, compound **3** and AuNPs/compound **3** composite. The absorption band of the as-prepared AuNPs was at approximately 520 nm (Fig. 5(a)). Compound **3** exhibited one major characteristic absorption band at 290–450 nm that is associated with the π–π^* transition of the π-conjugated benzenoid rings (Fig. 5(b)). The spectra of the AuNPs/compound **3** composite looked like a combination of those of as-prepared AuNPs and compound **3** (Fig. 5(c)). The absorption band at 520 nm, assigned to AuNPs was retained, so UV–vis revealed that not only did the AuNPs fail to grow into larger particles, but also they were well dispersed in the AuNPs/compound **3** composite following Paal–Knorr reaction in aqueous media using β-cyclodextrin as catalyst.

3.1.3. IR spectra

The compound **1**, compound **2** and compound **3** were investigated by IR spectroscopy. Fig. 6 shows the FT-IR results of compound **1**, compound **2** and compound **3**, and thereby confirms the structure of the *N*-substituted pyrrole derivatives obtained by Paal–Knorr reaction. The characteristic vibrations of compound **1** appear at 1600, 1499, 1300–1000 and 770–700 cm^{-1}, corresponding to the aromatic C—C stretching, C—N stretching of the pyrrole ring, aromatic C—H in-plane bending and aromatic C—H out-of-plane bending, respectively (Fig. 6(a)). The characteristic vibrations of compound **2** appear at 3386 and 790 cm^{-1}, corresponding to the N—H stretching and N—H wagging vibration of the amine group, respectively (Fig. 6(b)). The characteristic vibration of compound **3** appears at 1410 cm^{-1}, corresponding to the symmetrical stretching of the N=O bond (Fig. 6(c)). Moreover, the major characteristic bands observed in the spectra of compound **2** and compound **3** are similar to compound **1** indicating that the chemical structure of the *N*-substituted pyrrole backbone is same.

3.2. Electrical and humidity-sensing properties of humidity sensors made of N-substituted pyrrole derivatives films

Fig. 7 plots the impedance values of the compound **1**, compound **2**, compound **3** films as functions of relative humidity, and Table 1 summarizes the results concerning electrical resistance at 30% RH, sensitivity (defined as the slope of the logarithmic impedance ($\log Z$) as functions of %RH) and linearity (a correlation coefficient that is defined as the *R*-squared value of the fitted line from 30 to 90% RH). The measurements were made at 25 °C, an AC voltage of 1 V, and a frequency of 1 kHz. At low RH (<30%RH), the impedance values followed the order compound **2** < compound **1** < compound **3** (as indicated in the inset and Table 1), revealing that electron-donating (—NH_2) or electron-withdrawing (—NO_2) substituents that are attached to the benzene ring of compound **1** affect the electrical conduction of the compound **1**. Reynolds et al. [24] found that electron-donating substituents on 1,4-bis(2-furanyl)phenylene increased its electrical conductivity. Therefore, compound **2**, which has an effective electron-donating —NH_2 group, had a higher electrical conductivity than did compound **3,** which has an electron-withdrawing —NO_2 substituent [24,25]. The compound **1** film exhibited only a small change in impedance over the studied humidity range, undoubtedly owing to its hydrophobic property. Both compound **2** and compound **3** were more sensitive

www.cn.com

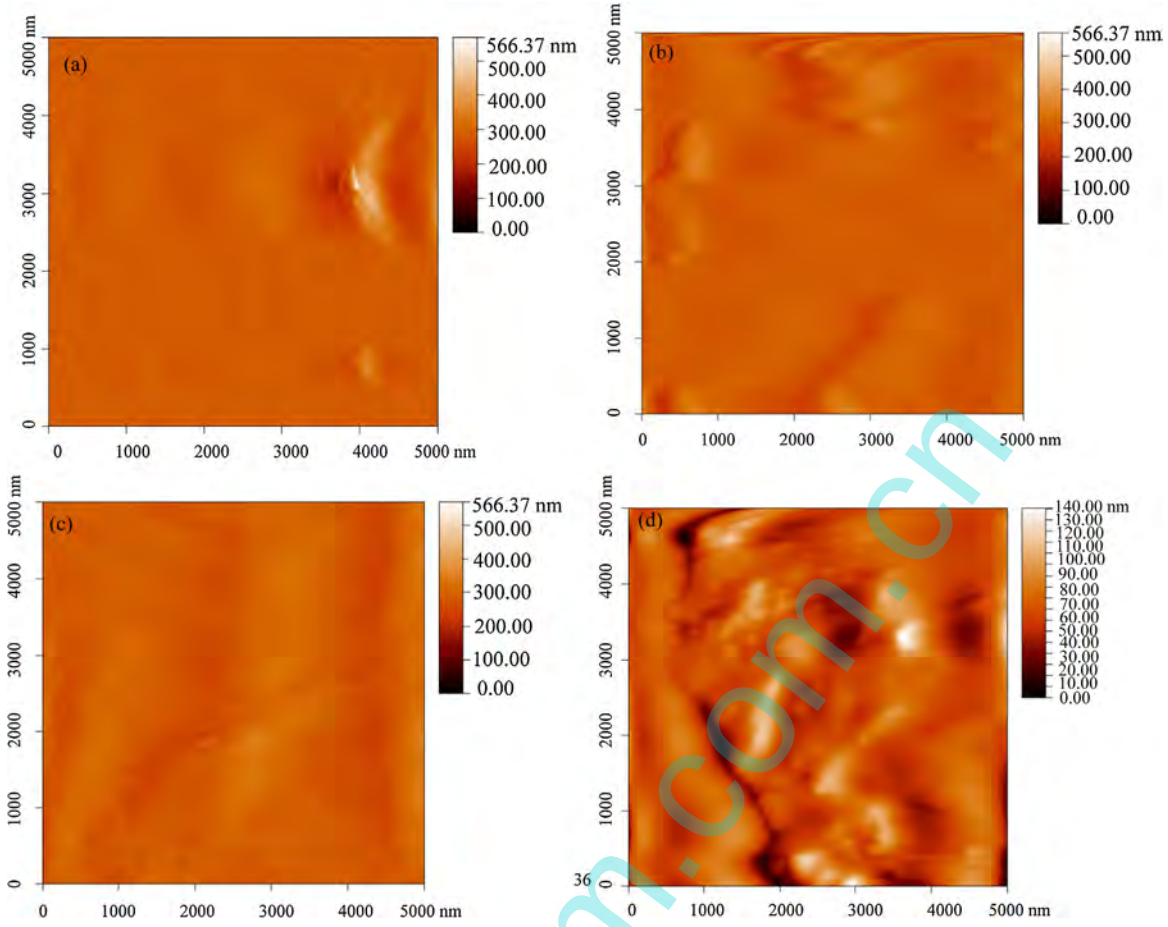

Fig. 4. AFM images of (a) compound **1**; (b) compound **2**; (c) compound **3** and (d) AuNPs/compound **3** films.

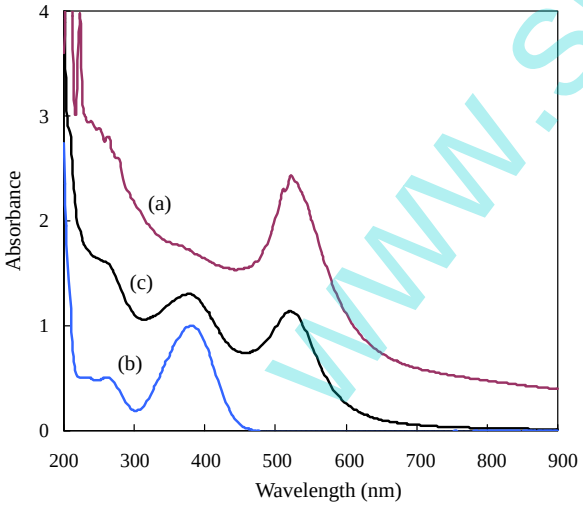

Fig. 5. UV–vis absorption spectra of (a) as-prepared AuNPs; (b) compound **3** and (c) AuNPs/compound **3**.

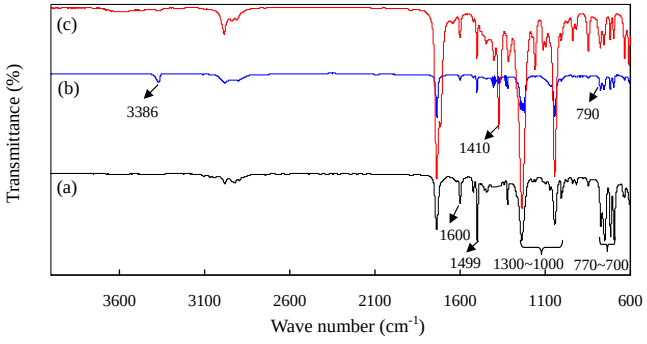

Fig. 6. IR spectra of (a) compound **1**; (b) compound **2** and (c) compound **3**.

than compound **1** (Table 1). AFM analysis (Fig. 4) demonstrates that the surface morphologies of the *N*-substituted pyrrole derivatives films varied very little. Therefore, the fact that the sensitivities of the both compound **2** and compound **3** films exceeded that of the compound **1** film was not related to their surface properties, but rather to the fact that when an $-NH_2$ group or an $-NO_2$ group was substituted onto the benzene ring of compound **1**, the local polarity was increased, causing strong adsorption of water molecules, enhancing the sensitivity of the compound **1** film. Furthermore, the sensitivities (slopes) of the compound **2** and compound **3** films to humidity were −0.0306 and −0.0518, respectively (Table 1), revealing that the response of the compound **3** film to humidity exceeded that of the compound **2** film. This observation was thought to follow from the fact that compound **3** had stronger a local polarity than compound **2**. Additionally, the compound **3** film had better linearity than the compound **2** film. Compound **3** had highest sensitivity and sensing linearity and a high electrical resistance, and so the compound **3** was used to fabricate AuNPs/*N*-substituted pyrrole derivative composite.

www.spm.com.cn

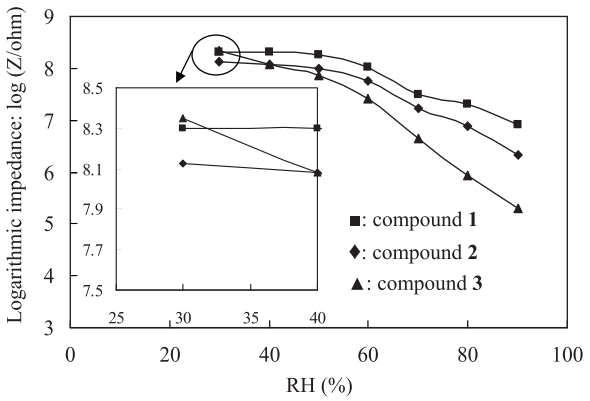

Fig. 7. Impedance versus relative humidity for humidity sensors that were made of compound **1**, compound **2** and compound **3** films coated on alumina substrates.

Table 1
Electrical resistance, sensitivity and linearity of humidity sensors that were made of *N*-substituted pyrrole derivatives films.

		Sensing curve	
Films	Impedance (MΩ)[a]	Sensitivity (log *Z*/%RH)[b]	Linearity (R^2)[c]
Compound **1**	201	−0.0245	0.9058
Compound **2**	134	−0.0306	0.9096
Compound **3**	223	−0.0518	0.9546

[a] The impedance of the *N*-substituted pyrrole derivatives at 30% RH.
[b] Sensitivity was defined as the slope of the logarithmic impedance versus relative humidity plot in the range 30 to 90% RH.
[c] Linearity was shown as the correlation coefficient of the logarithmic impedance versus relative humidity plot in the range 30 to 90% RH.

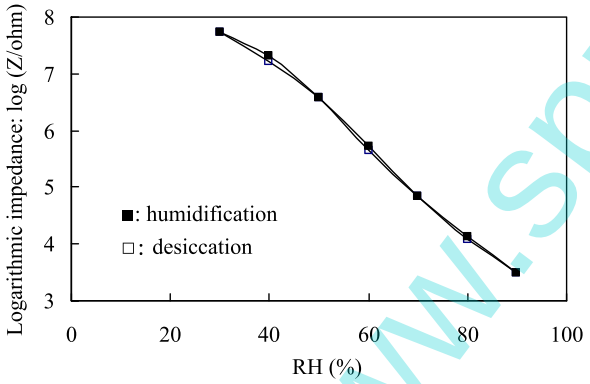

Fig. 8. Impedance versus relative humidity for AuNPs/compound **3** film on an alumina substrate, measured at 1 V, 1 kHz and 25 °C.

3.3. *Electrical and humidity-sensing properties of humidity sensors made of AuNPs/compound 3 composite*

To increase the electrical conductivity and sensitivity of the compound **3** film for practical use, the effect of adding AuNPs was studied. Fig. 8 plots the effects of adding AuNPs on the electrical and humidity-sensing properties of an AuNPs/compound **3** composite film for various relative humidities. The measurements were made at 25 °C, an AC voltage of 1 V, and a frequency of 1 kHz. The open symbols in the figure represent measurements made during desiccation, while the solid symbols represent those made during humidification. From 30 to 90% RH, the impedance fell from 10^7 to 10^3 Ω and the curves revealed a satisfactorily linear relationship ($Y = -0.0743\ X + 10.114$; $R^2 = 0.9951$) between log-impedance and RH. The hysteresis (between humidification and desiccation, measured over an RH range of 30–90%) was less than 1.0% RH. Incorporating AuNPs into compound **3** markedly

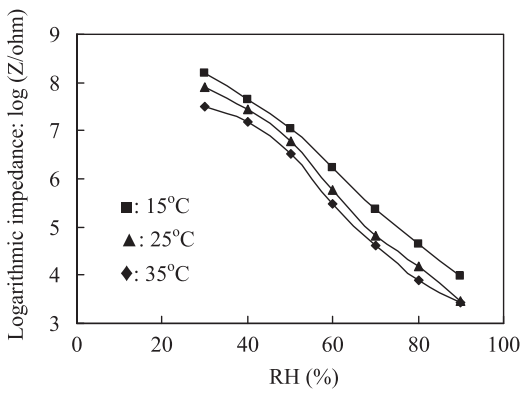

Fig. 9. Impedance versus relative humidity for AuNPs/compound **3** film on an alumina substrate at various temperatures, measured at 1 V and 1 kHz.

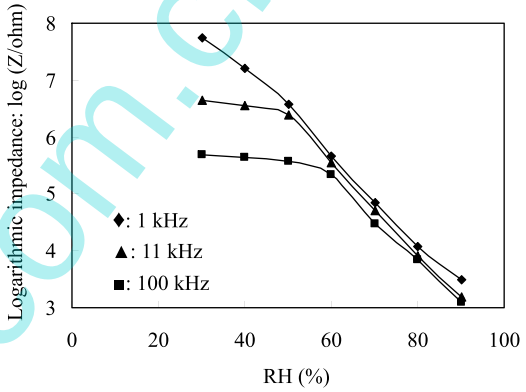

Fig. 10. Impedance versus relative humidity for AuNPs/compound **3** film on an alumina substrate at various frequencies, measured at 1 V and 25 °C.

reduced the impedance of the AuNPs/compound **3** composite film over a wide range of RH, suggesting higher sensitivity and improved linearity of the response curve. This result was reasonable because the AuNPs formed a new conductive path (improving conductivity) and AuNPs granules on the surface of AuNPs/compound **3**, presenting a high local charge density and a strong electrostatic field, indicating that water vapor molecules are more easily adsorbed on AuNPs/compound **3** than on compound **3** film, and thereby improving the sensitivity of AuNPs/compound **3** composite film. Therefore, the flexibility, humidity-sensing properties and sensing mechanism of the humidity sensor that was made of the AuNPs/compound **3** composite film was studied.

Fig. 9 plots the log-impedance of the humidity sensor versus temperature. As the temperature increased, the RH characteristic curve shifted to lower impedance. The mean temperature coefficient at 15–35 °C was −0.40% RH/°C over the humidity range 30–90% RH. Fig. 10 plots the dependence of the sensor impedance on the applied frequency; the impedance was measured at frequencies of 1, 11 and 100 kHz at a voltage of 1 V. The impedance of the humidity sensor decreased obviously with increasing the frequency at low RH, and the impedance difference among the working frequencies became gradually smaller with increasing RH. Because at a very high frequency the adsorbed water cannot be polarized (at RH < 60%), the dielectric phenomena does not appear [26]. The curve of impedance versus RH was most linear at 1 kHz. Fig. 11 plots the response and recovery of the humidity sensor that were measured of which measurements were made at 25 °C and 1 kHz. The response time ($T_{res.95\%}$) is defined as the time required for the impedance of the sensor to change by 95% of the maximum change following humidification from 13 to 90% RH. The recovery time

www.spm.com.cn

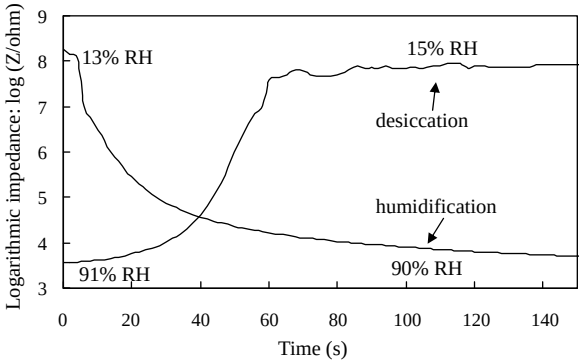

Fig. 11. Response-recovery properties of AuNPs/compound **3** film on an alumina substrate, measured at 1 V, 1 kHz and 25 °C.

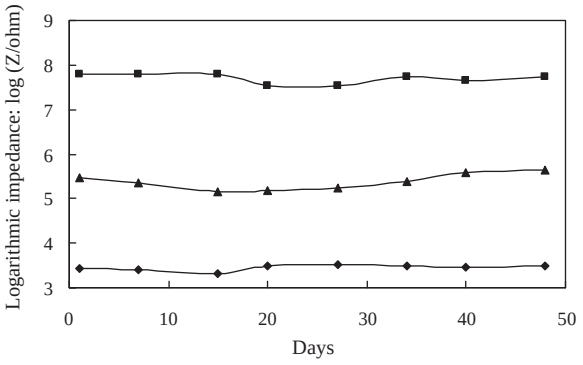

Fig. 12. Long-term stability of AuNPs/compound **3** film on an alumina substrate, measured at 1 V, 1 kHz and 25 °C. (■) 30% RH; (▲) 60% RH; (♦) 90% RH.

($T_{rec.95\%}$) is defined as the time taken for the sensor to recover 95% of the maximum change in impedance after desiccation from 91 to 15% RH. The response time ($T_{res.95\%}$) and recovery ($T_{rec.95\%}$) time of the sensor were 53 and 58 s, respectively. Fig. 12 plots the long-term stability. The humidity sensor impedance did not significantly vary for at least 48 days at the tested RH values of 30, 60, and 90% RH. Table 2 compares the humidity sensing properties of the presented humidity sensor with those in our earlier studies [7,8,27,28]. The presented humidity sensor that was made of AuNPs/compound **3** had a higher sensitivity and a smaller hysteresis than the sensor that was made of polymer electrolytes or their composites.

3.3.1. *Flexibility-related properties of humidity sensors made of AuNPs/compound **3** composite film*

Fig. 13 plots the flexibility-related characteristics of the AuNPs/compound **3** composite film that was used as a humidity sensor. The sensor response (S) was calculated according to $S = (\log Z_{30\%\,RH} - \log Z_{60\%\,RH})/\log Z_{30\%\,RH} \times 100\%$, ($\Delta Z/\log Z_{30\%\,RH} \times 100\%$), where $Z_{30\%\,RH}$ and $Z_{60\%\,RH}$ are the impedance of the flexible

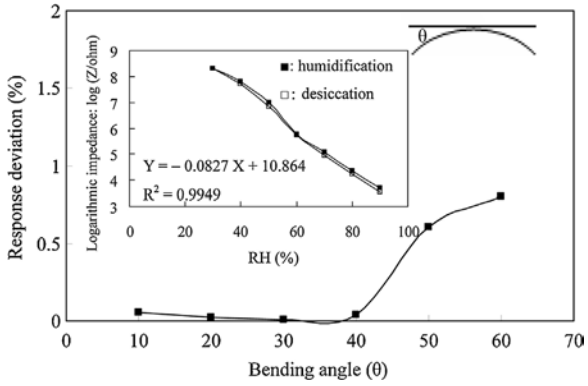

Fig. 13. Flexibility of AuNPs/compound **3** film on PET substrate, measured at 1 V, 1 kHz and 25 °C. Inset: impedance versus relative humidity for the flexible humidity sensor made of AuNPs/compound **3** film.

humidity sensor at 30 and 60% RH, respectively. At each bending angle, the sensor was exposed to 60% RH. The sensor response deviation (D) was calculated using the formula $D = (S_f - S_b)/S_f \times 100\%$), where S_f and S_b are the responses of the flat and bent flexible humidity sensor at 60% RH, respectively. When the sensor was bent downward at an angle of up to 60°, the response was changed by <1%. These results reveal that even under an applied stress, the sensor remained highly flexible and exhibited good electrical performance when it was bent. The inset plots the log-impedance of the flexible humidity sensor as a function of RH. The measurements were made at 25 °C, an AC voltage of 1 V, and a frequency of 1 kHz. The flexible humidity sensor exhibited high sensitivity and good linearity ($Y = -0.0827\,X + 10.864$; $R^2 = 0.9949$) between logarithmic impedance ($\log Z$) and RH in the range 30 to 90% RH, and a negligible hysteresis (within 1.0% RH) relative to that of a sensor that was fabricated on an alumina substrate.

3.4. *Sensing mechanism of humidity sensor made of AuNPs/compound **3** composite film*

Impedance spectroscopy is a powerful technique to understand the conduction mechanisms of humidity sensors. Therefore, the observed impedance plots (Fig. 14) were adopted to elucidate the transport process by ions in the conduction mechanism of the AuNPs/compound **3** composite film. The impedance measurements were made at frequencies from 50 Hz to 100 kHz, humidities at 30–90% RH, an AC voltage of 1 V and a temperature of 25 °C. In the impedance spectra, Z_r is the real part of the impedance Z, represented on the real axis, and Z_i is the imaginary part of Z, represented on the imaginary axis. At low humidity of 40% RH, a semicircular plot of film impedance was obtained. This film was modeled as an equivalent parallel circuit that included a resistor and a capacitor, as proposed elsewhere [29–31]. As RH increased (50% RH), a line appeared in the low frequency range, which became longer as RH further increased. The line finally became straight at

Table 2
Humidity sensor performance of this work compared with the literatures.

Sensing material	Working range (%RH)	Sensitivity ($\log Z$/%RH)[a]	Hysteresis (%RH)	Response time (s)	References
AuNPs/compound **3**	30–90	0.0743	<1	52	This work
TiO_2 NPs/polypyrrole	30–90	0.0306	<3	40	[7]
TiO_2 NPs/PPy/PMAPTAC[b]	30–90	0.0655	<2	30	[8]
PAMPS doped salts[c]	20–90	0.0260	< 8	60	[27]
PAMAM-AuNPs[d]	30–90	0.0450	< 2	40	[28]

[a] The sensitivity shown as the slope of the sensing curve in the working range.
[b] PMAPTAC: poly[3-(methacrylamino)propyl] trimethyl ammonium chloride.
[c] PAMPS: poly(2-acrylamido-2-methylpropane sulfonate).
[d] PAMAM: polyamidoamine.

www.sensorsportal.com

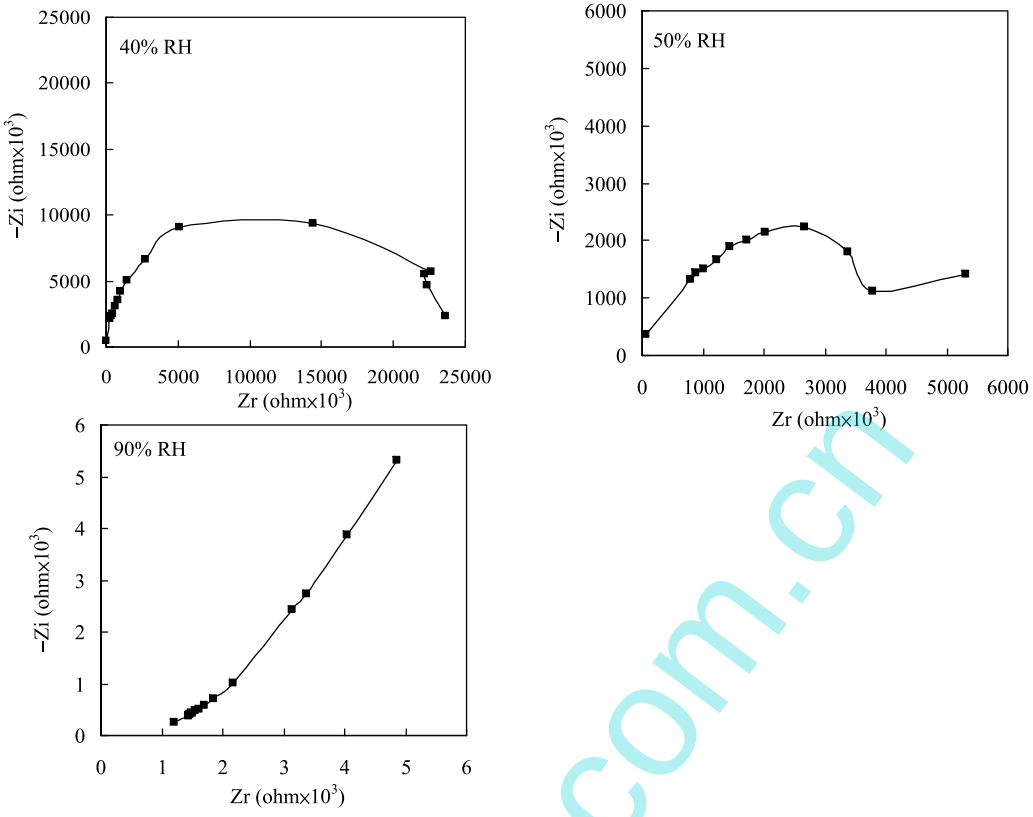

Fig. 14. Complex impedance plots of AuNPs/compound **3** film at various RHs.

90% RH. At high relative humidity, the plot of impedance entered two regions: a semicircle (at high frequencies) was associated with the AuNPs/compound **3** film intrinsic impedance and an inclined line (at low frequencies) represented Warburg impedance, which was established by the diffusion of ions (protons (H_3O^+) across the interface between the electrode and the AuNPs/compound **3** film [29,32,30,31]. Therefore, upon the adsorption of water, water molecules were physisorbed in a thin liquid layer formed around the AuNPs/compound **3** film, forming H_3O^+ ions by dissociation. As the relative humidity increased to 90% RH, the sorbed water acted as a plasticizer, increasing the mobility of the solvated ions (H_3O^+), which dominated the conduction in the sensor. Therefore, based on the complex impedance spectra, humidity-sensing by the AuNPs/compound **3** film depended on the ion transport mechanism.

4. Conclusions

The electron-donating (—NH_2) or electron-withdrawing (—NO_2) substituents on the benzene ring of compound **1** dominated the electrical and humidity-sensing properties (sensitivity) of the compound **1** film herein. The functionalization of compound **1** with an —NH_2 group or an —NO_2 group on the benzene ring can improve its surface properties and increase its sensitivity to humidity. Compound **3** had a higher sensitivity than the sensor made of compound **1** or compound **2**. Adding AuNPs into the compound **3** film provided conduction pathways, improving the conductivity, and thereby improving the sensitivity and linearity of the AuNPs/compound **3** film. The humidity sensor that was made of AuNPs/compound **3** film exhibited high sensitivity and good linearity ($Y = -0.0743X + 10.114$; $R^2 = 0.9951$) between logarithmic impedance ($\log Z$) and RH in the range 30 to 90% RH, negligible hysteresis (within 1.0% RH), high flexibility ($D < 1\%$), a smaller temperature effect between 15 and 35 °C (−0.4% RH/°C), a short response time (52 s), a short recovery time (58 s), and good long-term stability (48 days at least), measured at 1 V, 1 kHz and 25 °C. The humidity sensor had high flexibility ($D < 4\%$) when it was bent downward at an angle of up to 60°. The linearity of the humidity sensor depended on the applied frequency. Plots of the complex impedance of the AuNPs/compound **3** film at various RHs changed from semicircular to a liner with increasing RH. These results reflect the fact that ions contribute to the conductivity of the AuNPs/compound **3** film.

Acknowledgement

The authors thank the Ministry of Science and Technology (grant no. MOST 104-2113-M-034-001) of Taiwan for support.

References

[1] R.S. André, S.M. Zanetti, J.A. Varela, E. Longo, Synthesis by a chemical method and characterization of $CaZrO_3$ powders: potential application as humidity sensors, Ceram. Int. 40 (2014) 16627–16634.
[2] T. Fei, K. Jiang, S. Liu, T. Zhang, Humidity sensors based on Li-loaded nanoporous polymers, Sens. Actuators. B: Chem. 190 (2014) 523–528.
[3] K. Jiang, T. Fei, T. Zhang, Humidity sensing properties of LiCl-loaded porous polymers with good stability and rapid response and recovery, Sens. Actuators, B: Chem. 199 (2014) 1–6.
[4] S.W. Yun, J.R. Cha, M.S. Gong, Water-resistive humidity sensor prepared from new polyelectrolyte containing both photo-curable 4-styrylpyridinium function and thiol anchor, Sens. Actuators, B: Chem. 202 (2014) 1109–1116.
[5] Y. Sakai, Y. Sadaoka, M. Matsuguchi, Humidity sensors based on polymer thin films, Sens. Actuators, B: Chem. 35–36 (1996) 85–90.
[6] J.H. Cho, J.B. Yu, J.S. Kim, S.O. Sohn, D.D. Lee, J.S. Huh, Sensing behaviors of polypyrrole sensor under humidity condition, Sens. Actuators, B: Chem. 108 (2005) 389–392.
[7] P.G. Su, L.N. Huang, Humidity sensors based on TiO_2 nanoparticles/polypyrrole composite thin films, Sens. Actuators, B: Chem. 123 (2007) 501–507.
[8] P.G. Su, C.P. Wang, Flexible humidity sensor based on TiO_2 nanoparticles-polypyrrole-poly-[3-(methacrylamino)propyl] trimethyl ammonium chloride composite materials, Sens. Actuators, B: Chem. 129 (2008) 538–543.

www.sohn.com.cn

[9] A. Sun, Z. Li, T. Wei, Y. Li, P. Cui, Highly sensitive humidity sensor at low humidity based on the quaternized polypyrrole composite film, Sens. Actuators, B: Chem. 142 (2009) 197–203.
[10] S.K. Mahadeva, S. Yun, J. Kim, Flexible humidity and temperature sensor based on cellulose–polypyrrole nanocomposite, Sens. Actuators, A: Phys. 165 (2011) 194–199.
[11] Y. Li, C. Deng, M. Yang, A composite of quaternized and crosslinked poly(4-vinylpyridine) with processable polypyrrole for the construction of humidity sensors with improved sensing properties, Synth. Met. 162 (2012) 205–211.
[12] S.K. Shukla, Synthesis and characterization of polypyrrole grafted cellulose for humidity sensing, Int. J. Biol. Macromol. 62 (2013) 531–536.
[13] W. Geng, X. Li, N. Li, T. Zhang, W. Wang, S. Qiu, Humidity sensitivity of polypyrrole and polypyrrole/SBA-15 host-guest composite materials, J. Appl. Polym. Sci. 102 (2006) 3301–3305.
[14] W. Geng, N. Li, X. Li, R. Wang, J. Tu, T. Zhang, Effect of polymerization time on the humidity sensing properties of polypyrrole, Sens. Actuators, B: Chem. 125 (2007) 114–119.
[15] R. Ragno, G.R. Marshall, R.D. Santo, R. Costi, S. Massa, R. Rompei, M. Artico, Antimycobacterial pyrroles: synthesis, anti-mycobacterium tuberculosis activity and QSAR studies, Bioorg. Med. Chem. 8 (2000) 1423–1432.
[16] T. Watanabe, Y. Umezawa, Y. Takahashi, Y. Akamatsu, Novel pyrrole- and 1,2,3-triazole-based 2,3-oxidosqualene cyclase inhibitors, Bioorg. Med. Chem. Lett. 20 (2010) 5807–5810.
[17] S. Raghavan, K. Anuradha, Solid-phase synthesis of heterocycles from 1,4-diketone synthons, Synlett 2003 (2003) 711–713.
[18] H.R. Darabi, M.R. Poorheravi, K. Aghapoor, A. Mirzaee, F. Mohsenzadeh, N. Asadollahnejad, H. Taherzadeh, Y. Balavar, Silica-supported antimony(III) chloride as a mild and reusable catalyst for the Paal–Knorr pyrrole synthesis, Environ. Chem. Lett. 10 (2012) 5–12.
[19] A. Rahmatpour, Polystyrene-supported $GaCl_3$ as a highly efficient and recyclable heterogeneous Lewis acid catalyst for one-pot synthesis of *N*-substituted pyrroles, J. Organomet. Chem. 712 (2012) 15–19.
[20] F.J. Duan, J.C. Ding, H.J. Deng, D.B. Chen, J.X. Chen, M.C. Liu, H.Y. Wu, An approach to the Paal–Knorr pyrroles synthesis in the presence of β-cyclodextrin in aqueous media, Chin. Chem. Lett. 24 (2014) 793–796.
[21] S. Guo, E. Wang, Synthesis and electrochemical applications of gold nanoparticles, Anal. Chim. Acta 598 (2007) 181–192.
[22] H.D. Hill, C.A. Mirkin, The bio-barcode assay for the detection of protein and nucleic acid targets using DDT-induced ligand exchange, Nat. Protoc. 1 (2006) 324–336.
[23] P.G. Su, I.C. Chen, R.J. Wu, Use of poly(2-acrylamido-2-methylpropane sulfonate) modified with tetraethyl orthosilicate as sensing material for measurement of humidity, Anal. Chim. Acta 449 (2001) 103–109.
[24] J.R. Reynolds, A.D. Child, J.P. Ruiz, S.Y. Hong, D.S. Marynick, Substituent effects on the electrical conductivity and electrochemical properties of conjugated furanyl phenylene polymers, Macromolecules 26 (1993) 2095–2103.
[25] S. Pandule, A. Oprea, N. Barsan, U. Weimar, K. Persaud, Synthesis of poly-[2,5-di(thiophen-2-yl)-1*H*-pyrrole] derivatives and the effects of the substituents on their properties, Synth. Met. 196 (2014) 158–165.
[26] V. Bondarenka, S. Grebinskij, S. Mickevicius, V. Volkov, Thin films of poly-vanadium–molybdenum acid as starting materials for humidity sensors, Sens. Actuators, B: Chem. 28 (1995) 227–231.
[27] P.G. Su, W.C. Li, J.Y. Tseng, C.J. Ho, Fully transparent and flexible humidity sensors fabricated by layer-by-layer self-assembly of thin film of poly(2-acrylamido-2-methylpropane sulfonate) and its salt complex, Sens. Actuators, B: Chem. 153 (2011) 29–36.
[28] P.G. Su, C.C. Shiu, Electrical and sensing properties of a flexible humidity sensor made of polyamidoamine dendrimer-Au nanoparticles, Sens. Actuators, B: Chem. 165 (2012) 151–156.
[29] C.D. Feng, S.L. Sun, H. Wang, C.U. Segre, J.R. Stetter, Humidity sensing properties of Nafion and sol–gel derived SiO_2/Nafion composite thin films, Sens. Actuators, B: Chem. 40 (1997) 217–222.
[30] J. Wang, Q. Lin, T. Zhang, R. Zhou, B. Xu, Humidity sensor based on composite material of nano-$BaTiO_3$ and polymer RMX, Sens. Actuators, B: Chem. 81 (2002) 248–253.
[31] J. Wang, B.K. Xu, S.P. Ruan, S.P. Wang, Preparation and electrical properties of humidity sensing films of $BaTiO_3$/polystrene sulfonic sodium, Mater. Chem. Phys. 78 (2003) 746–750.
[32] G. Casalbore-Miceli, M.J. Yang, N. Camaioni, C.M. Mari, Y. Li, H. Sun, M. Ling, Investigations on the ion transport mechanism in conduction polymer films, Solid State Ionics 131 (2000) 311–321.

Biographies

Pi-Guey Su is currently a professor in Department of Chemistry at Chinese Culture University. He received his BS degree from Soochow University in Chemistry in 1993 and Ph.D. degree in Chemistry from National Tsing Hua University in 1998. He worked as a researcher in Industrial Technology Research Institute, Taiwan, from 1998 to 2002. He joined as an assistant professor in the General Education Center, Chungchou Institute of Technology from 2003 to 2005. He worked as an assistant professor in Department of Chemistry at Chinese Culture University from 2005 to 2007. He worked as an associate professor in Department of Chemistry at Chinese Culture University from 2007 to 2010. His fields of interests are chemical sensors, gas and humidity sensing materials and humidity standard technology.

Sih-Ru Chiu received a BS degree in Chemistry from Chinese Culture University in 2015. She entered the M.S. course of Chemistry at Chinese Culture University in 2015. Her main areas of interest are humidity-sensing materials.

Yu-Te Lin received a B.S. degree in Environmental Engineering from Da Yeh University in 2012. He entered the MS course of Chemistry at Chinese Culture University in 2014. His main areas of interest are humidity-sensing materials.

www.sp...